Navigation of Swarm Quadcopters in GPS-Denied Environment

Mina Mofid, Sherif Tabana, Mohamed El-Sayed, and Omar Hussein
Depart. of Computers Eng. and Artificial Intelligence, Military Technical College, Egypt
{mena.nady.177,sheriftabana09,mohamedkamal11,omarhussein98}@gmail.com

Supervisor: Sherif Hussein, and Tamer Attia
Military Technical College, Egypt

Abstract*—The integration of robotics into daily life applications is growing every day. Unmanned Aerial Vehicles (UAVs) are being extensively used for inspecting indoors, underground, surveying disaster sites, and tactical Search-and-Rescue missions. As these applications are mainly dependent on GPS signals, awareness increased of its two major shortcomings I) weak-to-no GPS signals at these locations, and II) ease at which the agents could be intentionally blocked from GPS access or communication signals at military or critical sites. Although this technology is still evolving, the movement toward developing algorithms that allow the operation of UAVs swarm is rising; to allow sharing of complicated tasks amongst the agents reducing the role of human operators. This paper discusses a reliable solution allowing a swarm of UAVs to traverse terrains in GPS-denied environments, using visual odometry to geo-localize. The proposed localization methodology comprises two stages: database preparation for the environment and onboard inference for real-time localization and navigation. The experimental results show that the proposed image-based localization succeeded in localizing the quadcopter and sharing its position with other quadcopters in the swarm formation. Additionally, the proposed swarm formation is able to control the leader and follower quadcopters to follow a predefined path with pre-set relative distance between the leader and follower.

I. Introduction

Autonomous independent navigation systems are necessary to safely operate UAVs in dangerous environments. Navigation may be obstructed by several means such as inspecting indoors and mining sites where these locations have poor GPS signals disrupting the agent from executing its mission. In addition, inspecting bridge structures and surveying disaster sites would have weak-to-no GPS signal. Furthermore, missions involving critical infrastructures sites and military Search-and-Rescue facing intended jamming targeting GPS and communication signals; these operations might be at high risk of failure [1].

Recently, the robotic swarm is an advanced technology to share a complicated task between agents to reduce the role of human operators and decision-making without direct intervention. Sets of swarm algorithms are used for controlling each agent in the swarm formation. These algorithms allow swarm agents to share tasks amongst themselves [2].

GPS-denied navigation depends on several methodologies. The capability of applying GPS-denied techniques is limited to onboard sensors available in which weight, cost, and computation power are needed in the field of UAVs.

Geolocating robotics is achieved by combining readings from velocity and rotation sensors to estimate the agent's position [3], yet sensors are susceptible to errors; consequently, the process of geolocation is complex and limited by mathematical modeling of input noise. LiDAR-Aided INS is a scan that fits aided Inertial Navigation Systems (INS) with a low-cost laser scanner, Light Detection and Ranging (LiDAR) used for environments in which GPS signal is degraded or denied [4]. Anchored Beacons are devices used with Indoor Positioning Systems (IPS) [5], indoor navigation seems more complex as indoor structures have many reflecting mediums that lead to multi-path and delay problems.

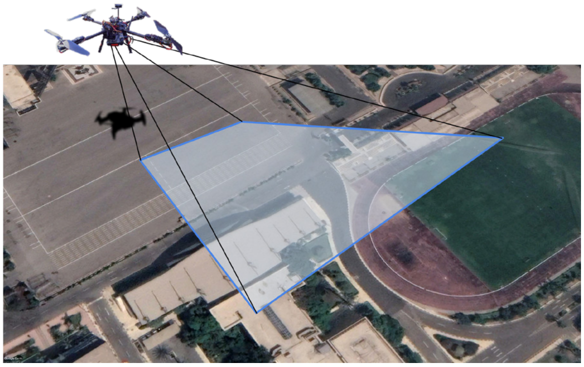

Fig. 1. The proposed image-based localization of the quadcopter.

Visual Odometry can work through visual feedback from a camera only, or both camera and other sensors. It estimates motion by monitoring changes in sequential images acquired by a vision system mounted on the agent. Features are selected and matched over successive frames to compute ego-motion, then the onboard computer processes the readings incoming from the sensors to perceive the optimal path to plan. The built-up database can be approached either by using an online satellite imagery application [6]–[8], or by pre-mapping the area to be traversed prior to executing a specific mission [9].

In this paper, we introduce an image-based localization approach for centralized control of swarm quadcopters using visual odometry of pre-mapped areas as shown in Figure 1. First, we present in section II-A localization discussing database preparation for the subjected environment and onboard inference for real-time localization and navigation. Then, in section II-B swarming using two agents and intercommunication. The experimental results are illustrated in section III including

**6th IUGRC International Undergraduate Research Conference,
Military Technical College, Cairo, Egypt, Sep. 5th – Sep. 8th, 2022.**

theoretical trials inside the laboratory and discussing the results, and on-field experiments with detailed procedures and outcomes. Finally, we conclude with future work in section IV.

II. Methodology

Developing a GPS-denied navigation system is a necessity as an alternative localization system to overcome GPS-related problems. In this section, we introduce the proposed approach for image-based localization of the quadcopter. We will analyze thoroughly our chosen methodology to implement such a system, first of all, In this section, we present our methodology, Primarily, divided into two parts: (A) Localization discussing stages; 1. Database preparation for the subjected environment and 2. Onboard inference for real-time localization and navigation, (B) Multi-agent Swarming.

A. Localization

The core of image-based localization is fetching and matching the pre-saved data at acceptable speed and accuracy. This method can be replaced by getting the imagery data from satellites (e.g., Google Earth) to overcome the need of traversing the environment in advance.

1) Database preparation: This process is divided into three steps;

- Pre-mapping,
- Filtering,
- Pre-processing.

In **Pre-mapping** process, the proposed quadcopter platform with onboard sensors is used to fly over the selected environment to capture the necessary imagery. The captured footage of the environments is saved to the Jetson Nano. During the pre-mapping process, the quadcopter maintained a constant speed, altitude, and fixed camera FOV while mapping and testing to avoid anomalies and mismatched features Figure 2.

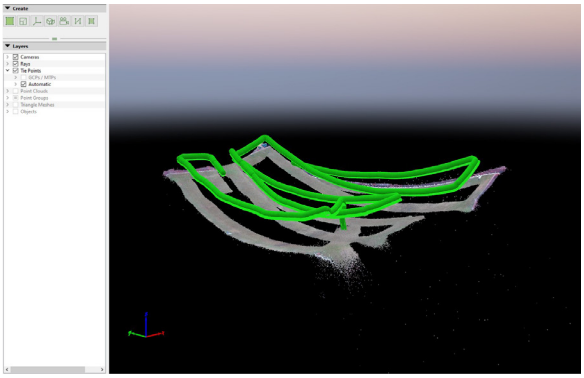

Fig. 2. Mapping of the Military Technical College (MTC) stadium.

Potential camera poses are calculated to obtain the altitude of the quadcopter and the angle of view that fit our task. Logitech C920 camera is fixed nadir with 78 FOV. The quadcopter is flying at 50 m altitude to get 55 meters of ground distance in the pictures and 1.5 m/s. Overlapping of 50% or above is recommended for mapping the field, while during database building; it is better to obtain overlapping 15% - 30%. The camera is set to record footage of 20 images/second with a resolution of 800*600 pixels of an average size of 600 Kilobytes each as shown in Figure 3, resulting in around 7.2 Gigabytes of storage needed for 10 minutes of mapping.

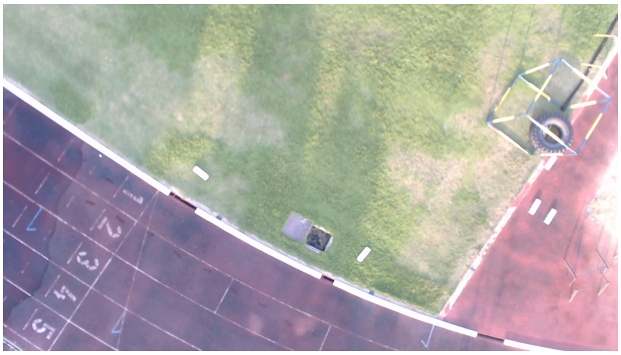

Fig. 3. Screen shot of the MTC's stadium from the UAV's onboard camera.

While in **Filtering** process, well-captured images covering most of the land area are selected from the whole database to reduce localization error and optimize onboard memory.

Finally, to reduce the onboard processing as **Pre-processing** step, features are extracted from each image locally [10], then attached to coordinates of the corresponding center point in Latitude and Longitude format, saved in a pickle file, and furtherly uploaded to the agent.

2) Onboard Inference: The database is then applied to the agent's Jetson Nano for further online processing during missions. The images are captured in real-time and compared with images at the approximate position from the database according to matched features. This process is divided into two steps; Matching strategy, and Pose Estimation.

In **Matching strategy**, the captured image is transformed into grayscale; it is furtherly compared to other images in the local database to find the highest match ratio, to conclude the correct orientation to rotate at, using OpenCV's homography built-in function; to map each point represented by a 3×3 matrix to its corresponding image, then determine its position, orientation, and altitude. Let us consider the first set of corresponding points $(x_1,\ y_1)$ in the first image and $(x_2,\ y_2)$ in the second image. Then, Homography **H** [11] maps them in the following way:

$$\begin{bmatrix} x_1 \\ y_1 \\ 1 \end{bmatrix} = H \begin{bmatrix} x_2 \\ y_2 \\ 1 \end{bmatrix} \begin{bmatrix} h_{00} & h_{01} & h_{02} \\ h_{10} & h_{11} & h_{12} \\ h_{20} & h_{21} & h_{22} \end{bmatrix} \begin{bmatrix} x_2 \\ y_2 \\ 1 \end{bmatrix}, \quad (1)$$

To calculate the Homography between two images, at least 4-point correspondences between them. An increasing number of points affects the output efficiency increasingly. But of course, not all mapped images and their corresponding in the database will be on the same plane, to overcome this problem; we implemented a photo-alignment algorithm by translating Homography's output matrix to Euler angles (Yaw, Pitch, and

Roll) allowing us to transform each captured image to a stated rotation position.

For **Pose Estimation**, the region of the match is calculated in the captured image and the local one, then, the difference between centers $(C_1,\ C_2)$ of both images is calculated $(\Delta X,\ \Delta Y)$ as shown in Figure 4. The latitude and Longitude of the local matched image are converted to Universal Transverse Mercator (UTM) to conclude the new target coordinate by the following equation,

$$\begin{bmatrix}X\\Y\end{bmatrix} = \begin{bmatrix}X_1\\Y_1\end{bmatrix} + D * \begin{bmatrix}|\sin(sign(\Delta X*\Delta Y)*\theta+|\alpha||*sign(\Delta X)\\ |\cos(sign(\Delta X*\Delta Y)*\theta+|\alpha||*sign(\Delta Y)\end{bmatrix}, \quad (2)$$

where D is the distance between C_1 and C_2 in meters, and θ is the angle between database image and North direction.

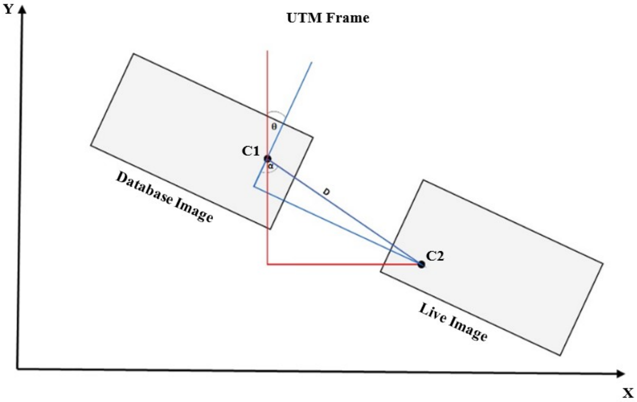

Fig. 4. Coordinate estimation from live imagery against database illustration.

B. Multi-agent Swarming

Various missions could be conducted in such applications with increasing benefits from each, swarm of UAVs aiding in optimizing time and maximizing performance during missions. Multiple formations can be implemented between a leader and follower agents [12], we go for centralized line formation as we currently test using only two quadcopters. Each agent is equipped with a 2.4 GHz Wi-Fi transceiver module; allowing initializing port communication between each. The leader agent is selected and pre-configured with a static IP address and port number to be accessed by the nearby agent. The mission starts when both confirm the mutual connection, leader initiates by sending a take-off command to the follower to maintain synchronization, and instant position and altitude are sent continuously to the follower agent to compute D-meter consistent difference between them as follows,

$$\begin{bmatrix}X\\Y\end{bmatrix} = \begin{bmatrix}X_{Leader}\\Y_{Leader}\end{bmatrix} - D * \begin{bmatrix}\sin(Yaw_{leader})\\ \cos(Yaw_{leader})\end{bmatrix}, \quad (3)$$

where $X,\ Y$ is in UTM coordinate.

III. Experimental Results

A quadcopter with a sensory system is used for evaluating the proposed image-based localization approach. The quadcopter's frame is Tarot 650 Carbon Fiber 4-Axis frame, the quadcopter is operated by a single 6-cell Lithium-ion Poly (LiPo) battery providing a maximum flight time of 10 minutes at a maximum speed of 27 Km/h; connected to Pixhawk flight controller and Jetson Nano for computer-vision tasks. Logitech C920 camera is fixed nadir (vertically downward) to the quadcopter to obtain the least distorted imagery while operating as shown in Figure 5.

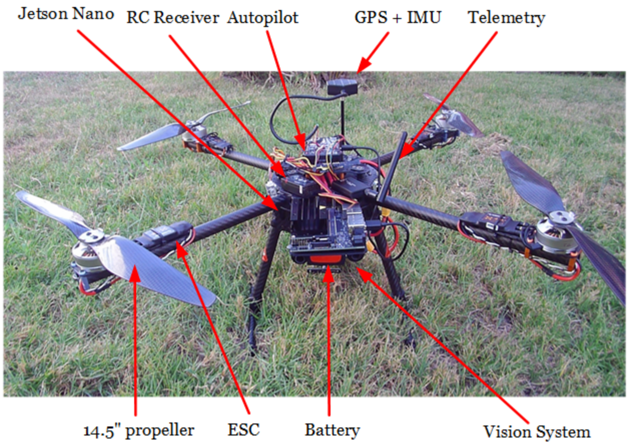

Fig. 5. The proposed quadcopter with vision system.

Hereby, we showcase the most productive tests, and results that added to the research and enhanced our algorithms. Firstly, the algorithm was tuned and verified offline in the laboratory, the database for the approximate flight location was built from imagery out of Google Earth at a suitable altitude, Figure 6 shows a sample from the whole database.

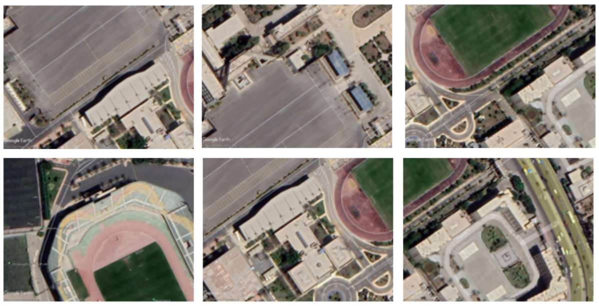

Fig. 6. Google Earth Imagery for the offline database.

To simulate the online footage, we did capture different photos at the same altitude with different orientations around the selected location. The algorithm explained in section II-A was applied to conclude actual and estimated error as shown in Figure 7.

Mapped estimates for the error tolerance at 150 meters varied between 2-5 meters as shown in Figure 8; validating

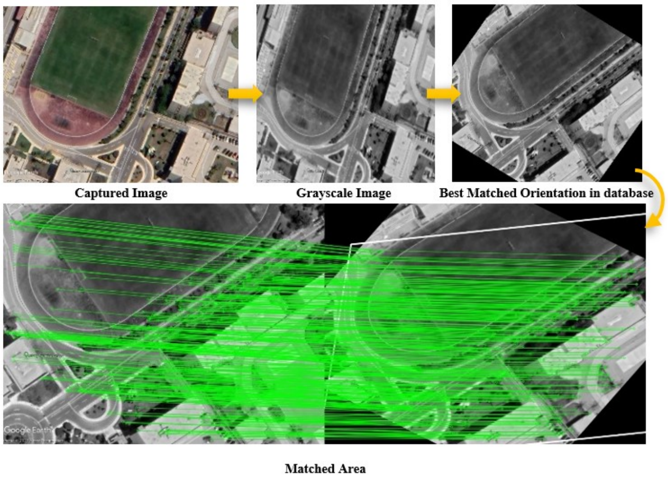

Fig. 7. The actual and estimated error for the matched area.

the efficiency of the pragmatic algorithm. For the first implementation of Scale-invariant feature transform (SIFT), code was executed in CPU single-thread mode in 13.4 seconds as for a 28-image database, to achieve more robust performance that could be used in real-life applications; code was modified to work in CPU multi-thread mode in 2.85 seconds as for the same database with the same output.

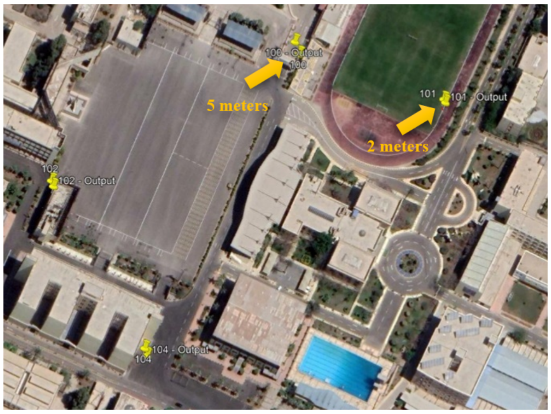

Fig. 8. Experimental error tolerance.

The SIFT algorithm meets the criteria proposed for this research; based on comparisons in [13] of SIFT versus Speeded-Up Robust Features (SURF) and Oriented FAST and rotated BRIEF (ORB) as shown in Table I in matching rate yielded from different-angled images, also, referring to other researchers in the same work-field, "SIFT is better than SURF in different scale images" [14] validate the point.

Two different experiments were conducted on both agents we work on with the same hardware, configurations, and mission path. The first trial was performed in the afternoon, and the second was performed in the evening to confirm the robustness of operation time for the agents as shown in Figure 9. Results showed that it is still not reliable to operate in weak lighting conditions, at least not with the same hardware used.

Table I
MATCHING RATE VERSUS ROTATION ANGLE [13]

Angle	0^o	45^o	90^o	135^o	180^o	225^o	270^o
SIFT	100	65	93	67	92	65	93
SURF	99	51	99	52	96	51	95
ORB	100	46	97	46	100	46	97

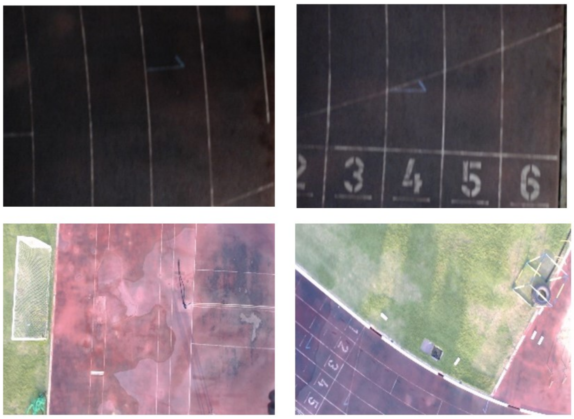

Fig. 9. Afternoon against night footage.

The output footage was selected to build a real-time database with the tuned algorithm, the mission was planned along the stadium's side and nearby area with a total covered distance of 110 meters; at 1.2 m/s and 20-meter altitude as shown in Figure 10.

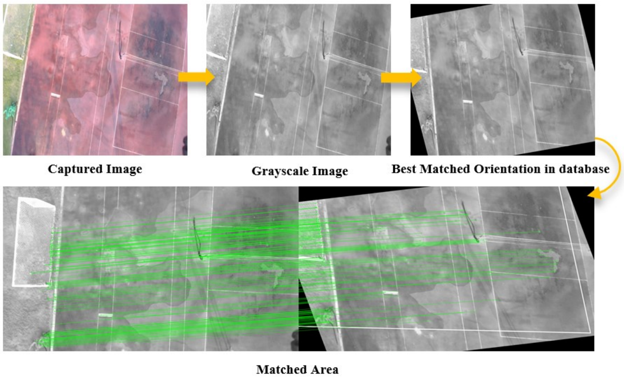

Fig. 10. Real-time imagery results.

The results show the variance in matched points rather than the offline database tests conducted at the laboratory; the lower altitude did influence the comparable features in both real-time and pre-mapped footage, offline tests yielded 2300 matched points compared to 390 points in the real-time test, though, error tolerance in the real-time experiment was 0.32 meters between estimated and actual target coordinates.

Additionally, the goal of this work is to investigate the applicability of swarming to increase its effectiveness in several applied fields. Both agents were configured to synchronize together before any mission as illustrated before. Where the planned experiment was conducted to set target coordinates for the leader agent to traverse a Z-shaped path across the MTC's stadium with a total distance of 120 meters at an altitude of 4 meters for the leader and 3 meters for the follower agent with a ground speed of 1.5 m/s while maintaining 15 consistent meters between the agents. The follower agent's algorithm depended on changing of ground speed to sustain the pre-set D-meters difference; by comparing instant distance in meters to the leader's current position, if the distance exceeded the pre-set relative distance, the follower's speed will be changed according to the following equation.

$$V_{follower} = V_{leader} + 0.1 * \Delta L, \tag{4}$$

Where ΔL is the position difference between the leader and the follower - D.

Figure 11 illustrates the path taken by the leader agent in red, followed by the follower agent in blue, where the follower succeeded to follow the leader agent according to the proposed formula in equation (4).

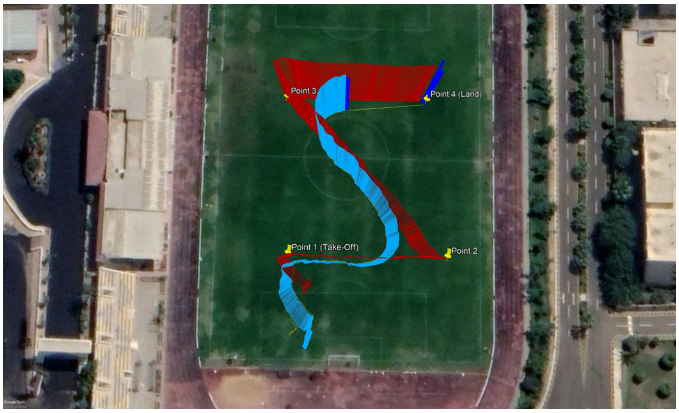

Fig. 11. Leader-follower paths; the leader is the red path while a follower is the blue path.

IV. Conclusions and Future Work

In this paper, we proposed a solution for GPS-denied UAVs swarm navigation that suits modern localization purposes. A swarm of two quadcopters with the necessary onboard sensory system is used for image-based localization and autonomous navigation. The proposed localization approach consists of two stages; database preparation for the environment and onboard inference for real-time localization and navigation. The experimental results demonstrate the ability of the proposed localization system in estimating the quadcopter's global position. Additionally, successful swarming tests were accomplished with acceptable results, and ready to be modified to include more than two agents simply. Across the different experiments using both agents, reasonable pose estimation accuracy was met, but not in the optimal time that will yield the best performance in the field. Future work will address this issue by introducing different hardware with high capabilities with tuning whilst modifying the current algorithm. Moreover, the algorithm is being tested to run in multi-threaded mode using the GPU of the onboard computer instead of the CPU. To widen fields of work for this application, a database should be built-up from rendered imagery by Google Earth rather than the necessity of pre-mapping the suspected field.

References

[1] G. L. Duckworth and E. J. Baranoski, "Navigation in gnss-denied environments: Signals of opportunity and beacons," in *Proceedings of the NATO Research and Technology Organization (RTO) Sensors and Technology Panel (SET) Symposium*, 2007.

[2] S.-J. Chung, A. A. Paranjape, P. Dames, S. Shen, and V. Kumar, "A survey on aerial swarm robotics," *IEEE Transactions on Robotics*, vol. 34, no. 4, pp. 837–855, 2018.

[3] N. Gageik, P. Benz, and S. Montenegro, "Obstacle detection and collision avoidance for a uav with complementary low-cost sensors," *IEEE Access*, vol. 3, pp. 599–609, 2015.

[4] J. Tang, Y. Chen, X. Niu, L. Wang, L. Chen, J. Liu, C. Shi, and J. Hyyppä, "Lidar scan matching aided inertial navigation system in gnss-denied environments," *Sensors*, vol. 15, no. 7, pp. 16 710–16 728, 2015.

[5] T. Varelas, A. Pentefoundas, C. Georgiadis, and D. Kehagias, "An ar indoor positioning system based on anchors," *MATTER: International Journal of Science and Technology*, vol. 6, no. 3, pp. 43–57, 2020.

[6] B. Patel, T. D. Barfoot, and A. P. Schoellig, "Visual localization with google earth images for robust global pose estimation of uavs," in *2020 IEEE International Conference on Robotics and Automation (ICRA)*. IEEE, 2020, pp. 6491–6497.

[7] A. Yol, B. Delabarre, A. Dame, J.-E. Dartois, and E. Marchand, "Vision-based absolute localization for unmanned aerial vehicles," in *2014 IEEE/RSJ International Conference on Intelligent Robots and Systems*. IEEE, 2014, pp. 3429–3434.

[8] C. Wu, F. Fraundorfer, J.-M. Frahm, J. Snoeyink, and M. Pollefeys, "Image localization in satellite imagery with feature-based indexing," in *XXIst ISPRS Congress: Technical Commission III*, vol. 37. ISPRS, 2008, pp. 197–202.

[9] S. Rady, A. Kandil, and E. Badreddin, "A hybrid localization approach for uav in gps denied areas," in *2011 IEEE/SICE International Symposium on System Integration (SII)*. IEEE, 2011, pp. 1269–1274.

[10] M. Yuvaraju, K. Sheela, and S. Rani, "Feature extraction of real-time image using sift algorithm," *International Journal of Research in Electrical & Electronics Engineering*, vol. 3, no. 4, pp. 01–07, 2015.

[11] E. Dubrofsky, "Homography estimation," *Diplomová práce. Vancouver: Univerzita Britské Kolumbie*, vol. 5, 2009.

[12] A. Tahir, J. Böling, M.-H. Haghbayan, H. T. Toivonen, and J. Plosila, "Swarms of unmanned aerial vehicles—a survey," *Journal of Industrial Information Integration*, vol. 16, p. 100106, 2019.

[13] E. Karami, S. Prasad, and M. Shehata, "Image matching using sift, surf, brief and orb: performance comparison for distorted images," *arXiv preprint arXiv:1710.02726*, 2017.

[14] D. Mistry and A. Banerjee, "Comparison of feature detection and matching approaches: Sift and surf," *GRD Journals-Global Research and Development Journal for Engineering*, vol. 2, no. 4, pp. 7–13, 2017.